

Supplementary Information for

Colorimetric and near infrared fluorescent detection of cyanide by a new phenanthroimidazole–indolium conjugated probe

Yi Zhang,[‡] Dehuan Yu,[‡] and Guoqiang Feng*

Key Laboratory of Pesticide and Chemical Biology of Ministry of Education, College of Chemistry, Central China Normal University, Wuhan 430079, P.R. China,

gf256@mail.ccnu.edu.cn

Table of contents:

1. Determination of the fluorescence quantum yield	Page 2
2. Additional data for sensing cyanide by probe 1	Page 2
3. Enlarged ¹ H NMR spectra changes of probe 1 with addition of CN ⁻	Page 5
4. Structure characterizations for the isolated 1-CN adduct	Page 6
5. Structure characterizations for probe 1	Page 7

1. Determination of the fluorescence quantum yield

The fluorescence quantum yields of probe **1** ($\Phi = 0.014$) and **1-CN** adduct ($\Phi = 0.034$) were determined in Tris·HCl buffer (10 mM, pH = 9.3, containing 50% MeOH, v/v) at 25°C, using quinine sulfate ($\Phi_f = 0.58$ in 1N H₂SO₄) as standard. The quantum yield was calculated using the following equation:

$$\Phi_x = \Phi_s (A_s F_x / A_x F_s) (n_x^2 / n_s^2)$$

where, A_x and A_s are the absorbance of the sample and the reference, respectively, at the same excitation wavelength, F_x and F_s are the corresponding relative integrated fluorescence intensities, and n is the refractive index of the solvent.

2. Additional data for sensing cyanide by probe 1

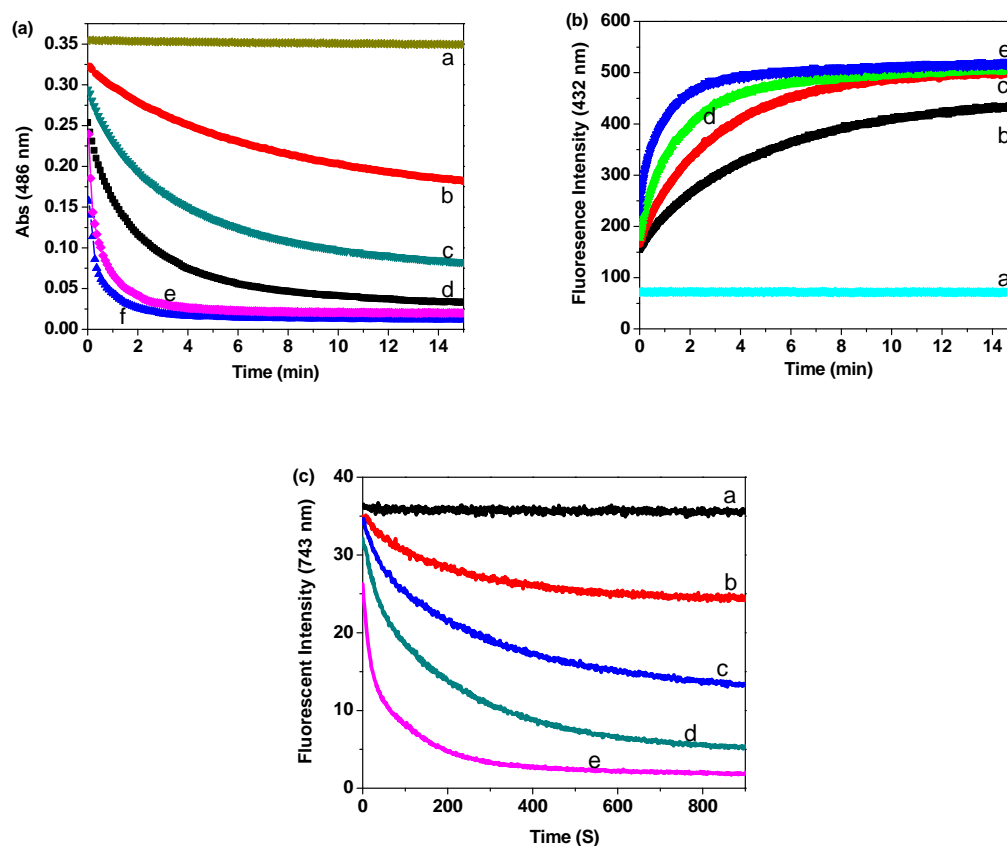


Fig. S1 (a) UV-vis kinetics of probe **1** (20 μM) monitored at 486 nm with different concentration of CN⁻ (a. 0 μM, b. 10 μM, c. 20 μM, d. 40 μM, e. 100 μM, f. 200 μM). (b) Fluorescent kinetics of probe **1** (20 μM) monitored at 432 nm (λ_{ex} : 380 nm) with different concentration of CN⁻ (a. 0 μM, b. 20 μM, c. 40 μM, d. 100 μM, e. 200 μM). (c) Fluorescent kinetics of probe **1** (20 μM) monitored at 743 nm (λ_{ex} : 480 nm) with different concentration of CN⁻ (a. 0 μM, b. 10 μM, c. 20 μM, d. 40 μM, e. 100 μM). All reactions were investigated in MeOH–Tris·HCl buffer (10 mM, pH = 9.3, 1 : 1, v/v) at 25 °C.

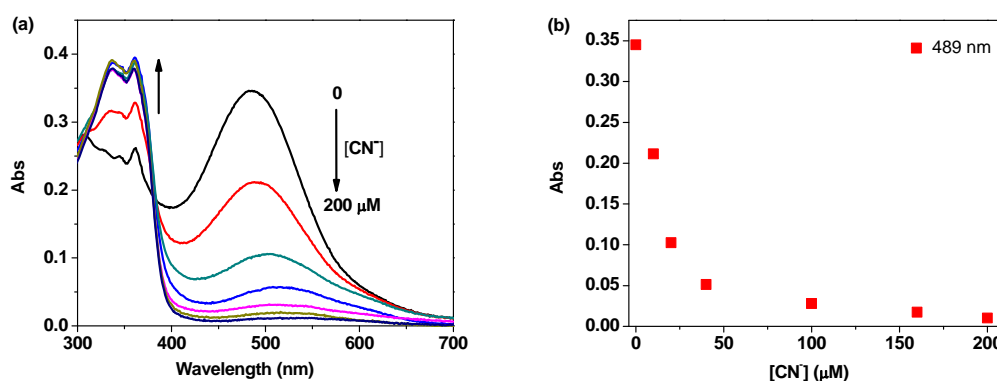


Fig. S2 (a) UV-vis spectra of probe **1** (20 μM) upon addition of 0, 10, 20, 40, 100, 160, 200 μM CN^- in MeOH-Tris-HCl buffer (10 mM, pH = 9.3, 1 : 1, v/v) at 25°C. (b) The absorbance intensity changes of probe **1** at 489 nm as a function of CN^- concentrations. Each spectrum were recorded 10 min after the addition of CN^- .

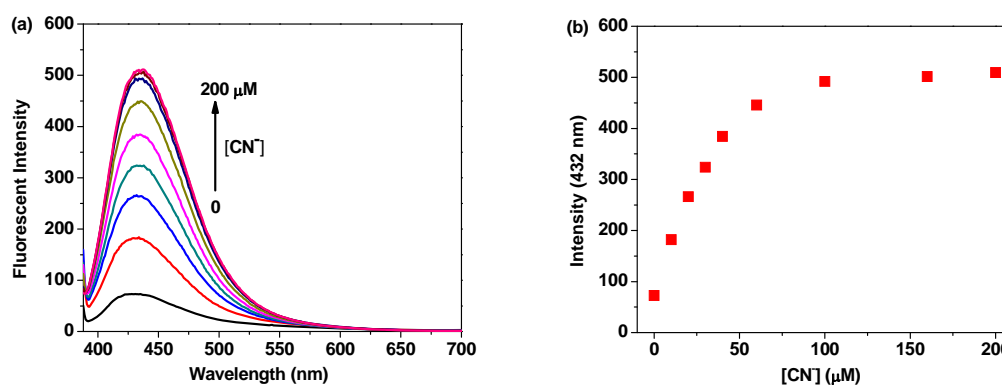


Fig. S3 (a) Fluorescence spectra changes of probe **1** (20 μM) upon addition of 0, 10, 20, 30, 40, 60, 100, 160, 200 μM of CN^- in MeOH-Tris-HCl buffer (10 mM, pH = 9.3, 1 : 1, v/v) at 25 °C. (b) Fluorescence intensity changes of probe **1** at 432 nm against $[\text{CN}^-]$ from 0-200 μM . Spectra data were recorded 10 min after the addition of CN^- with $\lambda_{\text{ex}} = 380$ nm, $d_{\text{ex}} = 5$ nm, $d_{\text{em}} = 10$ nm.

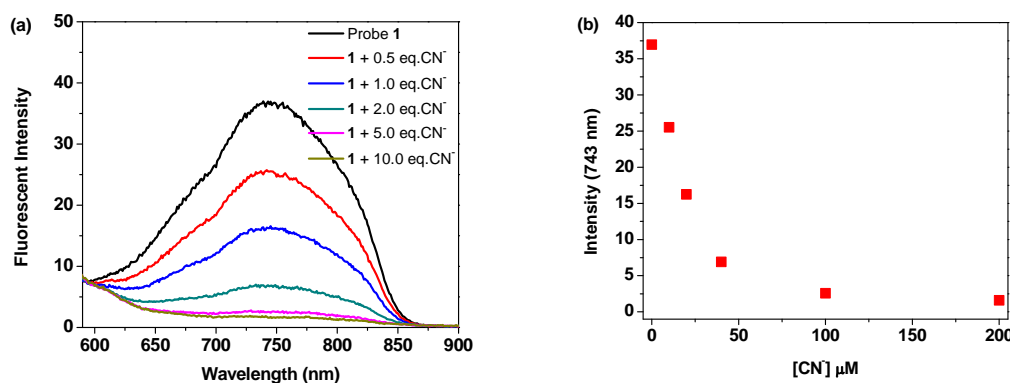


Fig. S4 (a) Fluorescence spectra changes of probe **1** (20 μM) upon addition of 0, 10, 20, 40, 100, 200 μM of CN^- in MeOH-Tris-HCl buffer (10 mM, pH = 9.3, 1 : 1, v/v) at 25 °C. (b) Fluorescence intensity changes of probe **1** at 743 nm against $[\text{CN}^-]$ from 0-200 μM . Spectra data were recorded 10 min after the addition of CN^- with $\lambda_{\text{ex}} = 380$ nm, $d_{\text{ex}} = 5$ nm, $d_{\text{em}} = 10$ nm.

200 μM CN^- in MeOH-Tris-HCl buffer (10 mM, pH = 9.3, 1 : 1, v/v) at 25 $^\circ\text{C}$. (b) Fluorescence intensity changes of probe **1** at 743 nm against $[\text{CN}^-]$ from 0-200 μM . Spectra data were recorded 10 min after the addition of CN^- with $\lambda_{\text{ex}} = 480$ nm, $d_{\text{ex}} = 10$ nm, $d_{\text{em}} = 10$ nm.



Fig. S5 (a) Color changes and (b) fluorescence color changes under a 365 nm UV light of probe **1** (20 μM) with 100 μM of different anions (from left to right: none, CN^- , S^{2-} , Cys, F^- , I^- , SCN^- , SO_4^{2-} , NO_3^- , HSO_4^- , N_3^- , Cl^- , NO_2^- , Br^- , N_3^- , H_2PO_4^- , HCO_3^- , PO_4^{3-} , CO_3^{2-} and ClO_4^- MeOH-Tris-HCl buffer (10 mM, pH = 9.3, 1 : 1, v/v) at room temperature.

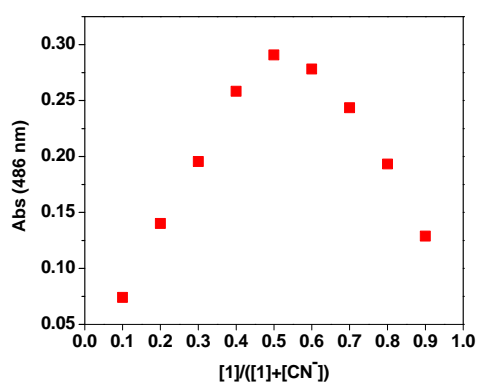
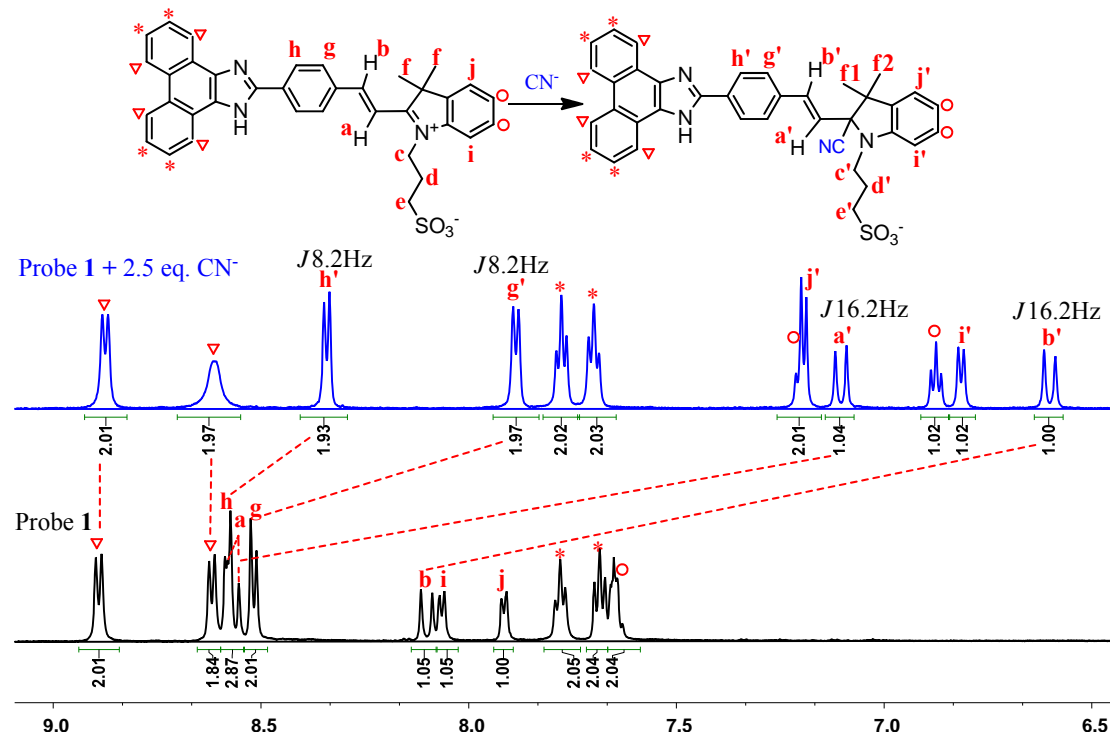
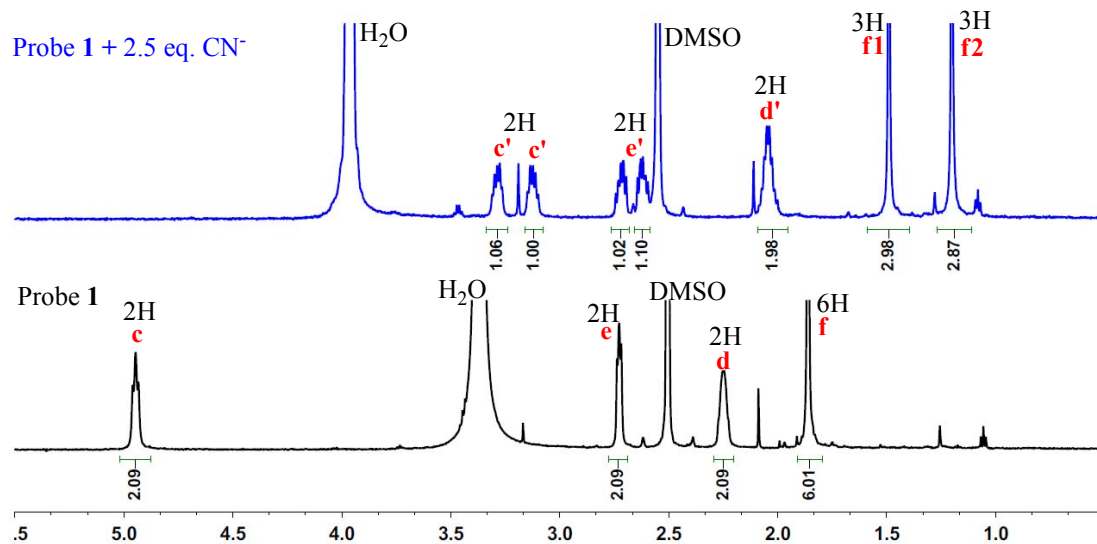


Fig. S6 Job's plot examined between probe **1** and CN^- . Total concentration of **1** + CN^- was kept constant at 50 μM .

3. Enlarged ^1H NMR spectra changes of probe 1 with addition of CN^-



(1) Aromatic protons signal change of probe 1 with addition of CN^-



(2) Aliphatic protons signal change of probe 1 with addition of CN^-

Fig S7. Enlarged ^1H NMR (600 MHz) spectra changes of probe 1 with addition of CN^- .

4. Structure characterizations for the isolated 1-CN adduct

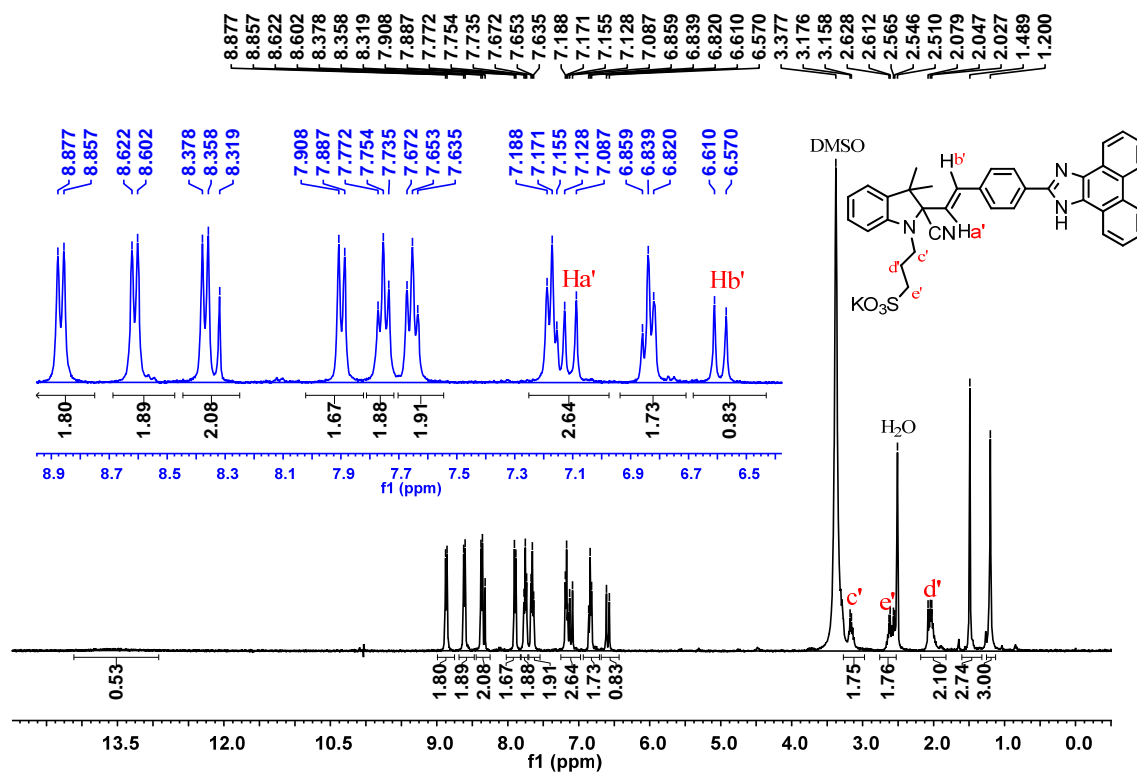


Fig. S8 ^1H NMR spectrum of the isolated probe 1-CN adduct in DMSO- d_6 (400 MHz)

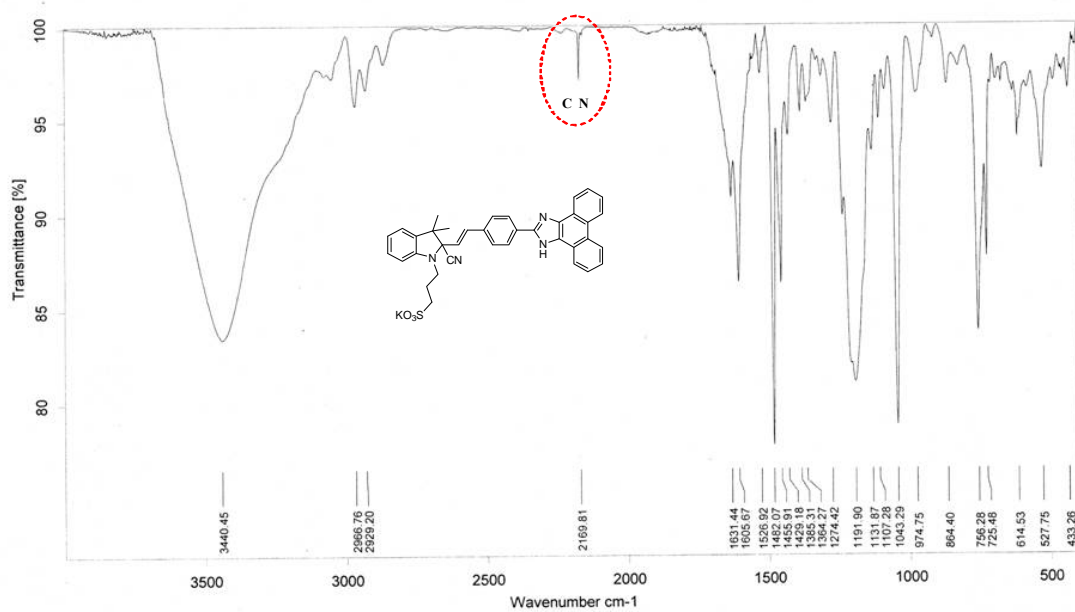


Fig. S9 IR spectrum of the probe 1-CN adduct

ZY-24-CN #824 RT: 5.35 AV: 1 SB: 659 0.71-4.25, 5.63-6.33 NL: 5.90E3
T: +c Full.ms [40.00-700.00]

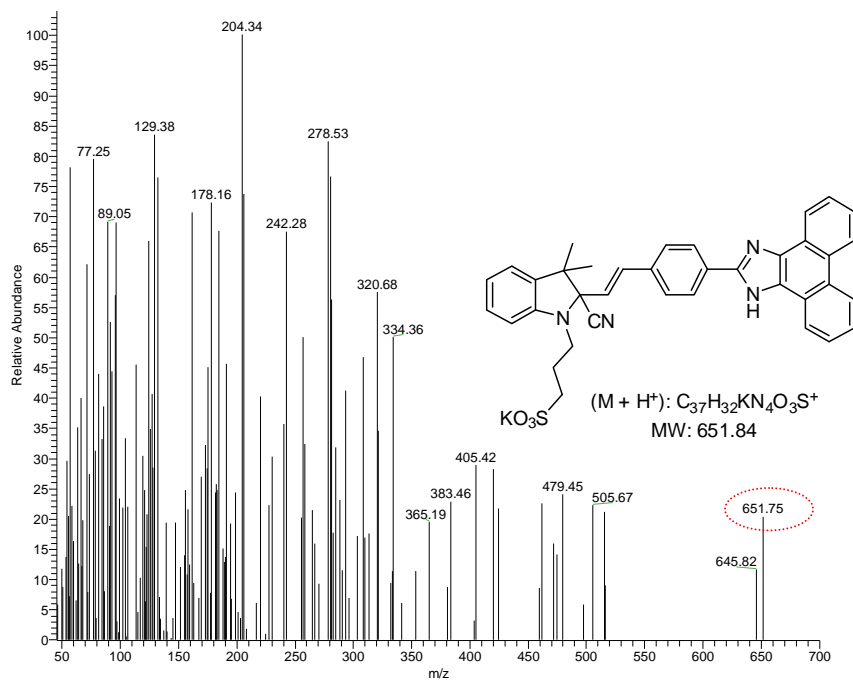


Fig. S10 EI-MS of 1-CN adduct.

5. Structure characterizations for probe 1

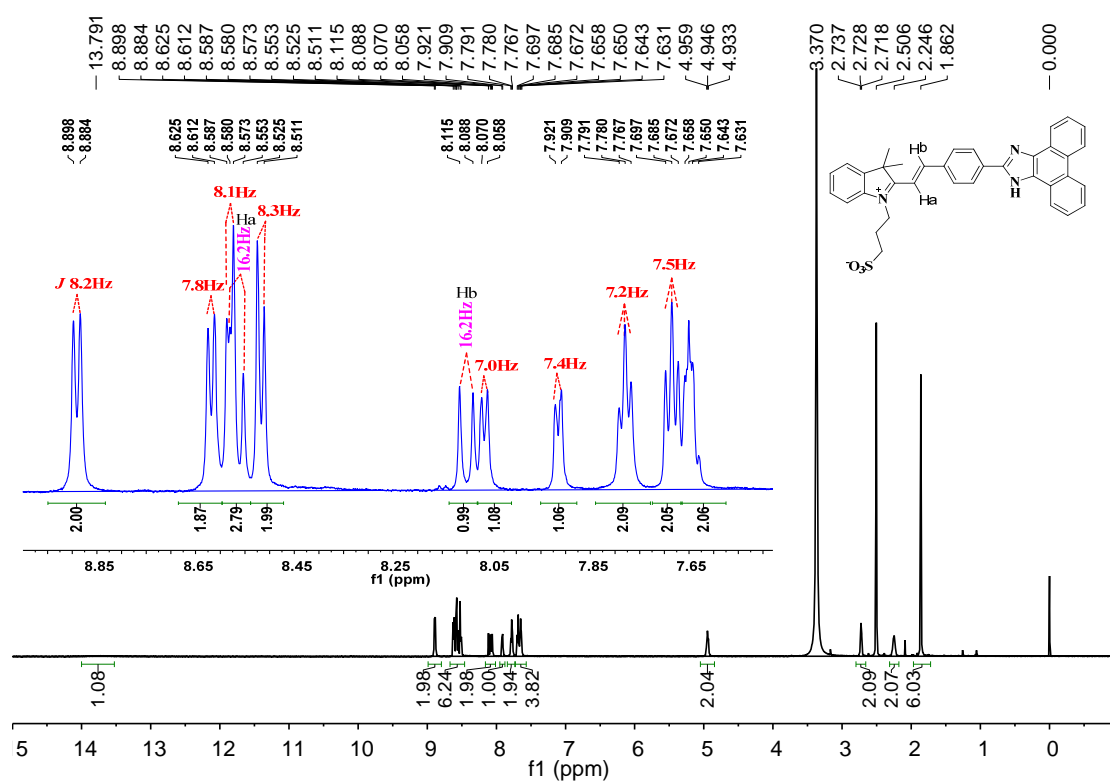


Fig. S11 ¹H NMR spectrum of probe 1 in DMSO-d₆ (600 MHz);

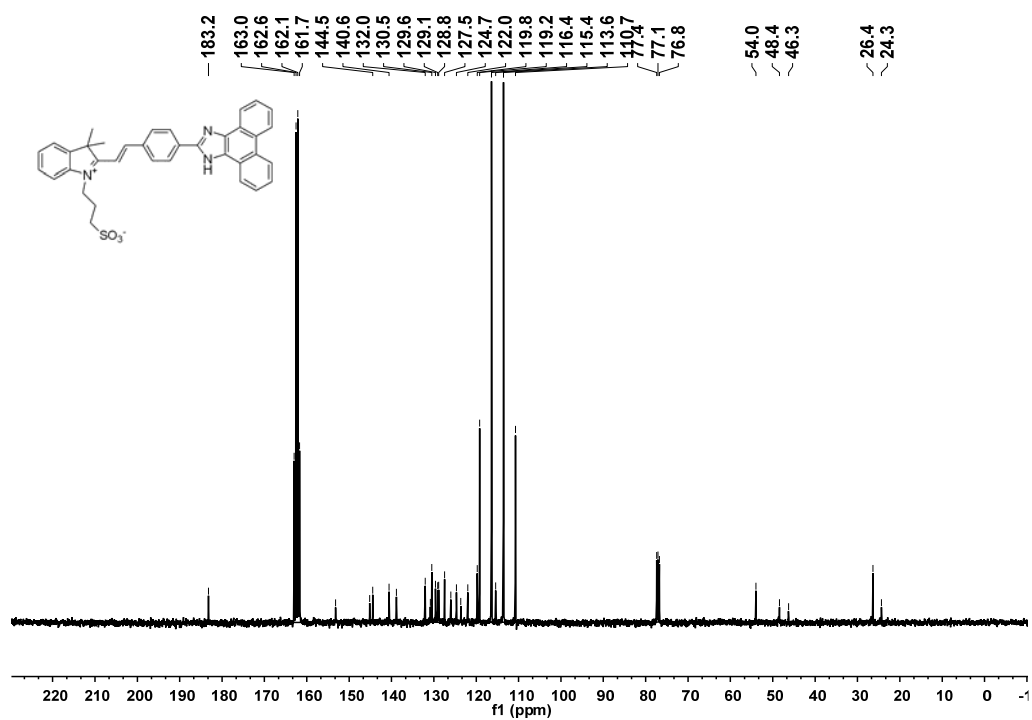


Fig. S12 ^{13}C NMR spectrum of probe 1 in a mixture of CF_3COOD and CDCl_3

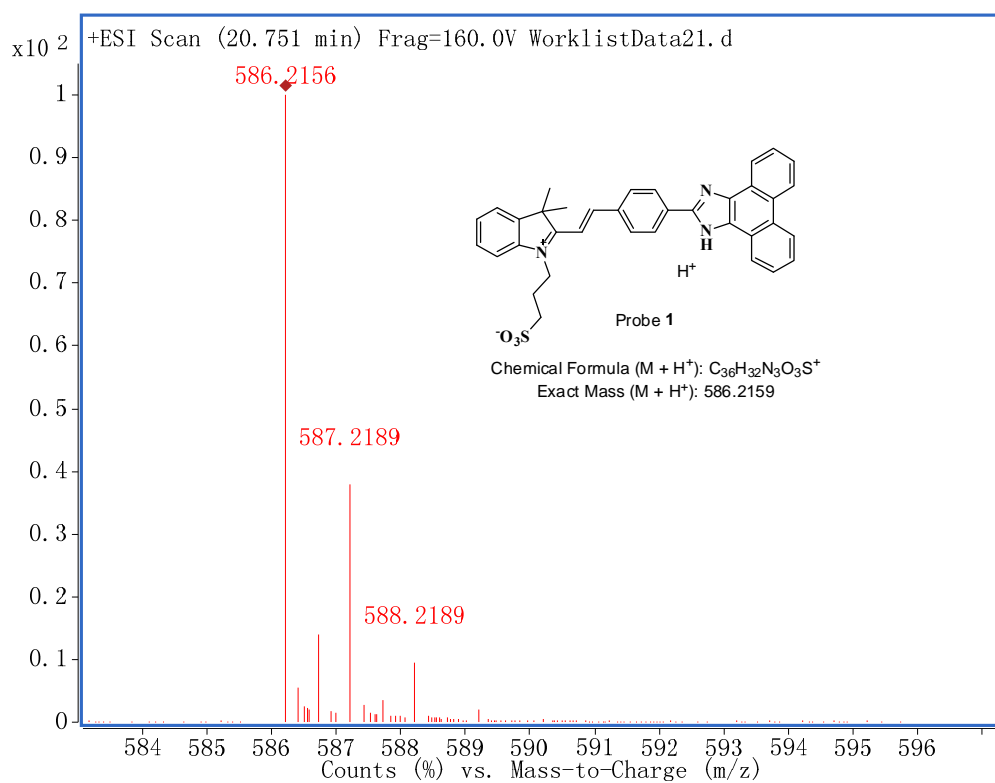


Fig. S13 HR-MS spectrum of probe 1

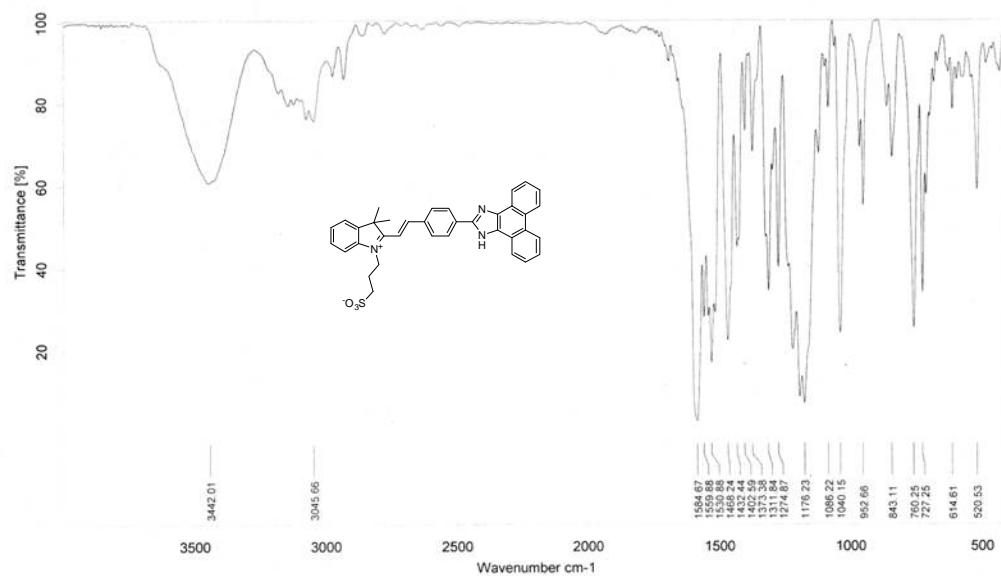


Fig. S14 IR spectrum of probe **1**